Genomics and Genetics 2020, 13(2&3): 33–43

Interleukin-6 and hepatocyte growth factor produce from chromosomal aberrant cholangiocarcinoma-associated fibroblasts

Suyanee Thongchot[1,2], Penkhae Utaijaratrasmi[1], Pranisa Jamjantra[1], Worapa Heepchantree[3], Kulthida Vaeteewoottacharn[4,5], Sopit Wongkham[4,5], Peti Thuwajit[1], Chanitra Thuwajit[1*]

[1]Department of Immunology, Faculty of Medicine Siriraj Hospital, Mahidol University, Bangkok 10700, Thailand
[2]Siriraj Center of Research Excellence for Cancer Immunotherapy (SiCORE-CIT), Faculty of Medicine Siriraj Hospital, Mahidol University, Bangkok 10700, Thailand
[3]Division of Medical Genetics, Office for Research and Development, Faculty of Medicine Siriraj Hospital, Mahidol University, Bangkok 10700, Thailand
[4]Faculty of Dentistry, Thammasat University, Bangkok 12120, Thailand
[5]Departments of Biochemistry, Faculty of Medicine, Khon Kaen University, Khon Kaen 40002, Thailand
[6]Liver Fluke and Cholangiocarcinoma Research Center, Khon Kaen University, Khon Kaen 40002, Thailand

**Corresponding author: cthuwajit@yahoo.com*

ABSTRACT

Cholangiocarcinoma (CCA)-associated fibroblasts (CCFs) have been identified as the cancer progression impact through the aberrant production of tumorigenic substances. This study is aimed to investigate the production of tumor-related cytokines from primary culture CCFs and their tumorigenic properties in context of CCA. Primary culture CCFs were isolated from fresh CCA tissues and verified by morphology, chromosomal pattern, and the expressions of fibroblast markers: vimentin (VIM), alpha-smooth muscle actin (ASMA); epithelial markers: cytokeratin 7 and 19 (CK7 and CK19); and periostin (PN). Migration induction of the conditioned-media (CM) from CCFs on CCA cells was shown by wound healing assay. The results revealed that all CCFs had the spindle-liked morphologies and the presence of VIM, ASMA and PN, but not CK19. Additionally, CCFs-CM induced migration of CCA cells. CCFs had aberrant chromosomal patterns including tetraploid and diploid chromosomes with deletion, amplification and translocation. The abnormal karyotypes were 92,XXYY; 46,X,-Y,+7; 46,XY,der(8)t(8;?); 92,XXYY,der(8)t(8;?),der(8)t(8;?); and 92,XX,-Y,-Y,+7,+7. In contrast, normal skin fibroblasts (NLFs) exhibited diploid chromosome with 50% had Y-chromosome deletion. Furthermore, upregulations of hepatocyte growth factor (HGF) and interleukin-6 (IL-6) with increased recruitment of CCF-CMs were observed. IL-6 and hepatocyte growth factor located on chromosome 7 showed increased expressions and IL-6 was confirmed the increment in more CCF-CMs. These observations provide the evidences that dysregulation of IL-6, a tumorigenic substance from CCFs, may be resulted from chromosomal aberrations. These data give us an experimental foundation for further studies to explore the mechanism underlining the involvement of fibroblasts in CCA progression.

Keywords: fibroblast; cholangiocarcinoma; migration; chromosomal aberration; interleukin-6

INTRODUCTION

The tumor stroma is a critical component of the tumor microenvironment comprises of several cell elements including chiefly cancer-associated fibroblasts, endothelial cells, and immune cells. It has crucial roles in tumor initiation, progression, and metastasis which support the fact that the novel treatment strategies should combine anticancer and antistromal agents (Valkenburg *et al.*, 2018). Several lines of evidences show that cancer-associated fibroblasts, a major cellular component of the stroma, have an important role in almost all steps of carcinogenesis and tumor progression in cholangiocarcinoma (CCA) (Thongchot *et al.*, 2018). The alpha-smooth muscle actin (ASMA)-positive expression of cancer-associated fibroblasts predicted unfavorable prognosis in intrahepatic CCA patients and showed correlation with presence of lymph node metastasis (Sha *et al.*, 2018).

Using SNP microarrays, fibroblasts isolated from pancreatic, breast and ovarian cancer tissues showed no evidences of chromosomal copy number changes (Qiu *et al.*, 2008) as well as fibroblasts extracted from paraffin-embedded cervical cancer tissues (Corver *et al.*, 2011). Though breast cancer-

Received 9 June 2020, Revised 12 July 2020, Accepted 4 August 2020

associated fibroblasts mainly had genomically stable cellular constituents, DNA copy number changes consisting of the whole arm of chromosomes 6p and 9p plus interstitial 4q loss were reported (Hosein *et al.*, 2010). Karyotyping of the same cancer-associated fibroblasts revealed further chromosomal abnormalities, which included clonal loss of chromosomes, chromosomal duplications, and less frequent chromosomal rearrangements. In contrast, no abnormalities were observed in non-tumor-associated fibroblast counterparts. Several studies have reported a high frequency of genetic aberrations such as gene copy number alterations, loss of heterozygosity (LOH), microsatellite instability and point mutations in tumor suppressor genes and oncogenes in several cancer-associated fibroblasts (Ishiguro *et al.*, 2006). In breast cancer, a significant association between cancer-associated fibroblasts loss of heterozygosity signature/allelic imbalance on chromosome 11 and tumor grading/regional lymph node metastasis was reported (Fukino *et al.*, 2007). In addition, frequent somatic mutations in *PTEN* and *TP53* were exclusively reported in the stroma of breast cancer (Jin *et al.*, 2010). The identification of DNA copy number in the stroma cells during cancer progression as the result of the selective pressure placed on the stroma by the tumor to foster a pro-oncogenic environment was reported (Pelham *et al.*, 2006). Though the presence or absence of clonally somatic genetic alteration and the chromosomal aberration in the tumor stroma has been controversial (Polyak *et al.*, 2009), this kind of studies in CCA-associated fibroblasts (CCFs) has not been explored.

In this study, we aimed to characterize the aberrant chromosomal patterns and tumorigenic induction properties of primary culture CCFs isolated from fresh CCA tissues. The tumorigenic cytokine production from CCFs was investigated and confirmed the increased production of interleukin-6 (IL-6) and hepatocyte growth factor (HGF). These findings may support the tumorigenic impact of CCFs in CCA through the cytokines produced from the chromosomal aberrant CCFs.

MATERIALS AND METHODS

Patient samples

Four CCA patients composing of two well-differentiated and two papillary histological types were freshly collected with a median age of 67.5 years (Table 1). Three were male and one case was female. Fresh surgical sterile (decoded) tissues were collected from CCA patients undergone liver hepatectomy at Srinaharind Hospital, Faculty of Medicine, Khon Kaen University, Thailand. The sample collection procedure was approved by the Human Ethics Committee, Khon Kaen University (#HE521209). All patients were asked to write the inform consent according to the approval form.

Isolation of cholangiocarcinoma-associated fibroblasts

Fresh CCA tissues of around 0.5-1.0 mm^3 were submerged in 2X antibiotic-containing DMEM (Gibco BRL, Grand Island, NY, USA) with 10% fetal bovine serum (FBS) (Thermo Fisher Scientific, Inc., Waltham, MA) for 30 to 60 min to reduce microbial contamination during the process of sample collection and transfer. The samples were rinsed with 1X phosphate buffer saline (PBS) and cut into small pieces (1-2 mm^3). Fresh complete medium, 10% FBS-containing DMEM (Gibco BRL, USA) with 1X penicillin (100 U/ml) and streptomycin (100 µg/ml), amphotericin B (5 mg/ml) and HEPES (20 mM) (Thermo Fisher Scientific, Inc.), was used to wash out the cell debris. Then, the tissues were digested with 1,000 U/ml collagenase (Calbiochem, Billerica, MA, USA) and 0.1 mg/ml DNase I (Sigma-Aldrich, St. Louis, MO, USA) for 3 h, and the digested tissues were filtered through 100 µm and 70 µm nylon meshes. The cell suspensions were plated onto rat tail collagen-coated plates (5 µg collagen/cm^2; Sigma-Aldrich, MO, USA) containing complete media and let them sticky to the surface at 37°C in CO_2 incubator. After fibroblast-like cells were protruded from the underneath of the tissues, trypsinization of the adhered cells was performed with 0.25% trypsin/EDTA. The complete medium was replaced every 2-3 days. Two to three more trypsinization were performed when the cells grew to reach the confluency of the culture ware. This allowed the decontamination of epithelial cells. Cultures at around passage 5^{th} to 17^{th} as possible were used for the studies for cell identification and determining the biological characteristics. Normal skin fibroblasts (SFs) and non-tumorigenic liver fibroblasts (NLFs) were also cultivated using the methods mentioned above from skin at the incision area of the hepatectomized patients (HE no. 490143) and the adjacent grossly looked normal liver area of the cancer mass, respectively.

Table 1 Patient demographic data.

No.	Patient code	Age (y)	Sex	Tumor size (cm)	Histological type	Vascular invasion	LN metastasis
1	B149	63	M	5x4x5	WD	+	-
2	C093	72	F	6x6x4	Pap	-	-
3	C095	79	M	7.5x7x6		+	+
4	C096	79	F	8x8x7	WD	+	-

WD: well differentiated type, Pap: papillary type

Karyotypic analysis

CCFs in log phase at around 80-90% confluency were added with 100 µl colchicine (0.25 µg/µl) for 4 h. The cells were gently blown with a pipette and washed by Hank Balance Salt solution. Cells were collected by centrifugation of the cell suspension at 1,000 rpm for 10 min and the supernatant was removed. Then cells were trypsinized by 0.25% trypsin/0.1% EDTA and spread evenly across the cell surface in collection tube. The 0.075 M KCl hypotonic solution was added to the cells for 10 min twice. Then cells were fixed with fixative agent (methanol : acetic acid at 3:1) and centrifuge at 1,000 rpm for 10 min for 3 times. Cell suspension was dropped directly onto dry slides. The slides were air dried and then stained for Q-banding with quinacrine solution. Then the metaphases were scanned by program Metafer version 3.6 (MetaSystems, Altlussheim, Germany) for screening the number of chromosomes. Chromosomal aberration was analyzed by the expert as mentioned in ISCN 2009. Karyotyping was performed by program Ikaros version 5.3 (MetaSystems, Germany).

Immunofluorescence staining

Around 4,000 cells were plated into 96-well plate and 24-h cultured period was allowed for cell adhesion. The attached cells were then fixed with 4% paraformaldehyde (Sigma-Aldrich, St. Louis, MO, USA). Non-specific binding was blocked by incubating cells with 1% bovine serum albumin in 1X PBS for alpha smooth muscle actin (ASMA), 5% FBS in 1X PBS for vimentin (VIM) and cytokeratin 19 (CK19). The primary antibodies as following were used: 1:100 mouse anti-human CK19 (SC-6278, Santa Cruz Biotechnology Inc., Dallas, TX, USA), 1:500 mouse anti-human VIM (SC-6260, Santa Cruz Biotechnology Inc.), 1:200 mouse anti-human ASMA (Sigma-Aldrich, St. Louis, MO, USA), and 1X PBS was used as the negative control in place of the primary antibody. The duration time for each primary antibody was 3 h at RT. After washing with 1X PBS, goat anti-mouse IgG-Cy3 (Jackson ImmunoResearch Laboratories Inc., West Grove, PA, USA) was applied into the cells for 1 h at RT. Nucleus was stained with 1:1,000 Hoechst 33258 (Invitrogen Corporation, Carlsbad, CA, USA). The color signals were detected under fluorescence microscope.

PCR and reverse transcription-real time PCR

The conventional PCR was performed in order to investigate the level of *PN* expression in CCF and several types of CCA cell lines. This is to ensure that the primary culture fibroblasts have *PN* expression as previous report shown in the CCA tissues. The 50 ng of cDNA was used to perform in the PCR reaction of 25 µl containing 1X PCR buffer, 2.5 mM $MgCl_2$, 0.2 mM dNTPs, 2 U *Taq* polymerase, and 0.1 µM for each forward and reverse primer. One cycle of 95°C for 10 min was performed to eradicate the secondary structure and induce denaturation of DNA. Then the 40 PCR cycles of 95°C for 15 s, 60°C for 15 s and 72°C for 30 s were done. The PCR products were analyzed in 1.5% agarose gel electrophoresis.

RNA extraction from the fibroblasts was performed once the cells had reached about 90% confluence. Total cellular RNA was prepared using Trizol reagent (Gibco BRL, NY, USA) according to the manufacturer's directions. The cDNA was produced by the reverse transcription system using AMV reverse transcriptase (Promega, Fitchburg, WI, USA). Fifty ng of cDNA was used in the PCR reaction containing 1X PCR buffer, 3.5 mM $MgCl_2$, 0.2 mM dNTPs, 0.08 U *Taq* polymerase, 0.5X SYBR green, 0.04 mM each forward primer and reverse primer. Sequences of PCR primers are shown in Table 2. To avoid the errors of the amount of input cDNA in each reaction, the expression of *β-actin* was measured as the internal control. The RT-PCR

reactions were performed in LightCycler® 480 system (Roche Molecular Systems, Inc., Schweiz, Switzerland). The obtained Cp was used to calculate the folding of altered expression level to that of negative control by the relative quantification formula ($2^{-\Delta Cp}$).

Conditioned-media collection

Conditioned-media (CM) of all fibroblasts were collected by growing fibroblasts in fibroblast-complete medium for 2 days until cells reached about 90% confluency. Then cells were washed twice with 1X PBS and incubated in 10% FBS DMEM with 20 mM HEPES for 24 h. CMs were collected and centrifuged to remove debris. The CMs were sterile filtered and stored at -80ºC until used.

Wound healing assay (Migration assay)

Five thousand KKU-213 CCA cells were cultured in each well of the 6-well plate. The 48-h culture at 37°C in CO_2 incubator was allowed for cell adhesion. When cells reach 100% confluency, a pipette tip was used to scratch the surface of cell culture at the middle of the well and followed by washing three times with 1X PBS to get rid of the unattached cells. The scratched cells were then treated with either complete medium or different types of CCF-CMs or CCA-CM. The scratching areas indicated by reference line were recorded at the beginning and at the end of treatment including 6, 12, 24, and 48 h. The migration efficiency was determined as a wound healing of the scratching area which calculated by the following formula:

% Wound healing = (wound space at 0 h - wound space at the end of treatment) x 100 / wound space at 0 h

Immunohistochemistry staining of PN in CCA tissue

Paraffin-embedded tissues were used and antigens were retrieved in 10 mM sodium citrate buffer pH 6.0 at 95 °C for 40 min and endogenous peroxidase was blocked in 3% H_2O_2 in absolute methanol for 30 min. After blocking non-specific binding with 2% BSA in Tris-HCl pH 7.6 for 20 min, 1:10,000 dilution of rabbit anti-human PN (Biovendor, Heidelberg, Germany) was applied to the sections at room temperature overnight, followed by anti-rabbit Envision$^+$ System-HRP labeled polymer (Dako, Santa Clara, CA, USA) for 30 min at room temperature. The immunoreactive signal was developed by 3,3’ diaminobenzidine (DAB; Sigma, MO, USA) and counterstained with hematoxylin. The signal was checked under light microscope (IX71 Olympus, Waltham, MA).

Statistical analysis

The difference of data between the test and the control condition in this studied was analyzed by mean ± SD of three independent experiments. The statistically significant difference was performed using one-way ANOVA Student t-test with *p*-value of less than 0.05.

Table 2 Primer sequences used in this study.

Gene	Forward Primer (5’ to 3’)	Reverse Primer (5’ to 3’)	Size (bp)	Accession no.
PN	cactctttgctcccaccaat	tcaaagactgctcctcccata	157	AY140646
VIM	caggtagaccagctaaccaa	tgccagagacgcattgtca	152	NM_003380
CK7	gatgctgcctacatgagcaa	gggagcgactgttgtcca	160	NM_005556
CK19	agctagaggtgaagatccgcgac	cagattgtcgatctgcaggacaa	155	NM_002276.4
ASMA	aggaaggacctctatgctaacaat	aacacataggtaacgagtcagagc	379	NM_001613.2
IL-6	cgggaacgaaagagaagctcta	ggcgcttgtggagaaggag	68	NM_000600
HGF	ggctggggctacactggattg	ccaccataatccccctcacat	90	NM_000601.4
β-actin	cacactgtgcccatctacga	ctccttaatgtcacgcacga	162	X00351

RESULTS

Characterization of fibroblast-related markers in primary culture CCA fibroblasts (CCFs)

The isolated primary culture CCFs initially showed bi- or multi-polar morphology and then finally had long spindle-like shape when reaching confluency (Figure 1A). This shape was sustained throughout the passages used in the whole experiments in this study. No differences between the morphologies of CCFs, SF and NLF (Figure 1A). Fibroblast cultures maintained the phenotypic properties of activated or myofibroblasts as the real time PCR results indicated the very low detection levels of *CK7* and *CK19* in CCFs compared to high expression levels in CCA cell lines including KKU-213, KKU-214, OCA17, KKU-055, KKU-156 and KKU-139 (Figure 1B). The very high level of *VIM* expression was detected in CCFs whereas its very low expression was observed in all CCA cell lines. The immunocytochemistry staining confirmed the total absence of CK19 in all CCFs in comparison to the positive control CK19-positive KKU-213 CCA cell lines. The filamentous pattern of VIM staining was indicated in CCFs which implied the mesenchymal properties of these CCFs as different from the homogenous cytoplasmic staining pattern of VIM in CCA cell lines. In addition, ASMA was detected positively in all CCFs and NLF which indicated the activated fibroblasts phenotype. In contrast, very faint signal of ASMA was detected in normal SFs (Figure 1C).

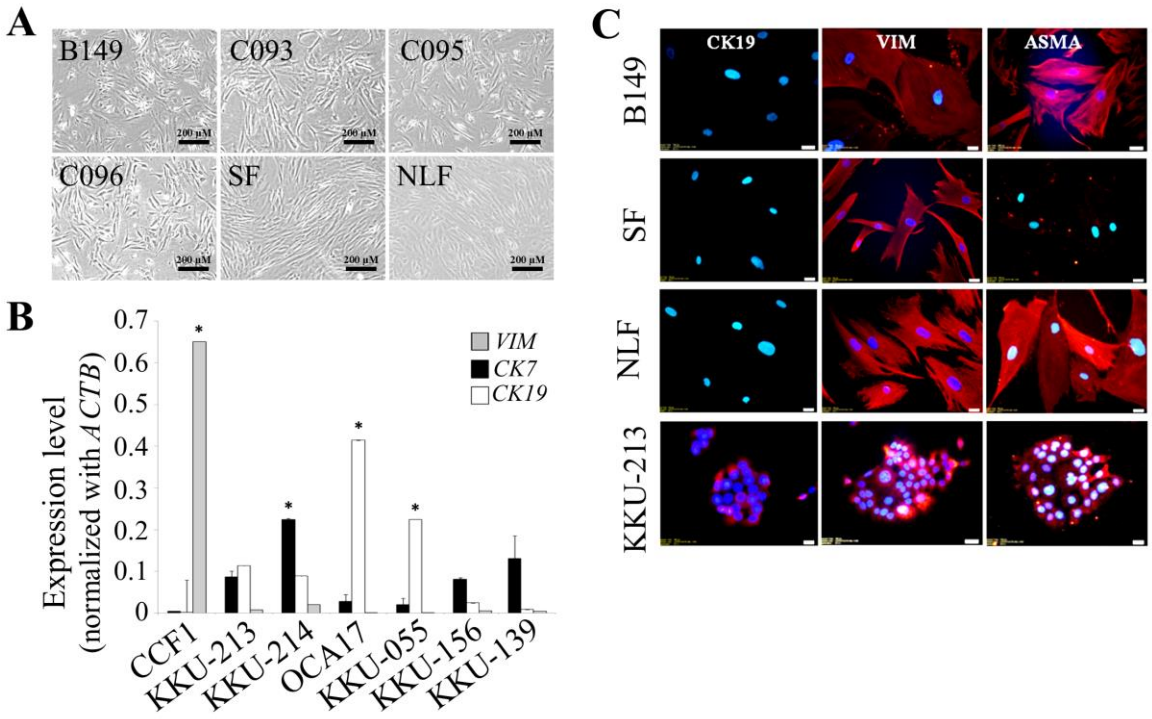

Figure 1 Characterization of primary culture CCFs. **(A)** Four CCFs (B149, C093, C095 and C096) were isolated from different CCA patients. The photographic pictures were taken from the inverted microscope under phase contrast mode in comparison to skin fibroblast (SF) and normal liver fibroblast (NLF). Magnification of 100x. Bars represent 200 µm. **(B)** Expression levels of mesenchymal and epithelial genes in primary culture CCF (B149). Graphs represent mean ± SD of gene expression level in term of $2^{-\Delta Cp}$ using the level of *ACTB* as the internal control. The levels of *CK7*, *CK19*, and *VIM* in CCFs were shown in comparison to those detected in six CCA cell lines. **(C)** Immunocytochemical analysis of the protein markers in primary culture CCFs. All four CCFs cells were immunoassayed for CK19, VIM, and ASMA using specific antibodies and Cy3-conjugated secondary antibodies. KKU-213 CCA cell line was used as the positive control of CK19 expression. Hoechst was used for nuclear staining in all conditions. Magnification of 400x. Bars represent 20 µm. *$p<0.05$.

Karyotypic pattern of CCFs

Two CCFs were sent for karyotypic analysis using three independent sample preparations. All CCFs, NLF and SF were from male patients. Among the total of 331 metaphase cells, the results showed that most of CCFs had 2n chromosome (83%, 275/331), while around 17% of CCFs showed tetraploid chromosomes (Table 3). This was opposed to that of NLFs that all these cells showed normal diploid chromosome, even though half of them had deletion of Y-chromosome. The completely normal karyotype was observed in SFs. The karyotypic pattern of CCFs revealed most of cells (64.2%) had aberrant chromosomes including 92,XXYY (26%), 46,X,-Y,+7 (24.7%), 46,XY,der(8)t(8;?) (8.6%), 92,XXYY,der(8)t(8;?),der(8)t(8;?) (3.7%), and 92,XX,-Y,-Y,+7,+7 (1.2%). The pictures of aberrant chromosomes of CCFs were exhibited (Figure 2).

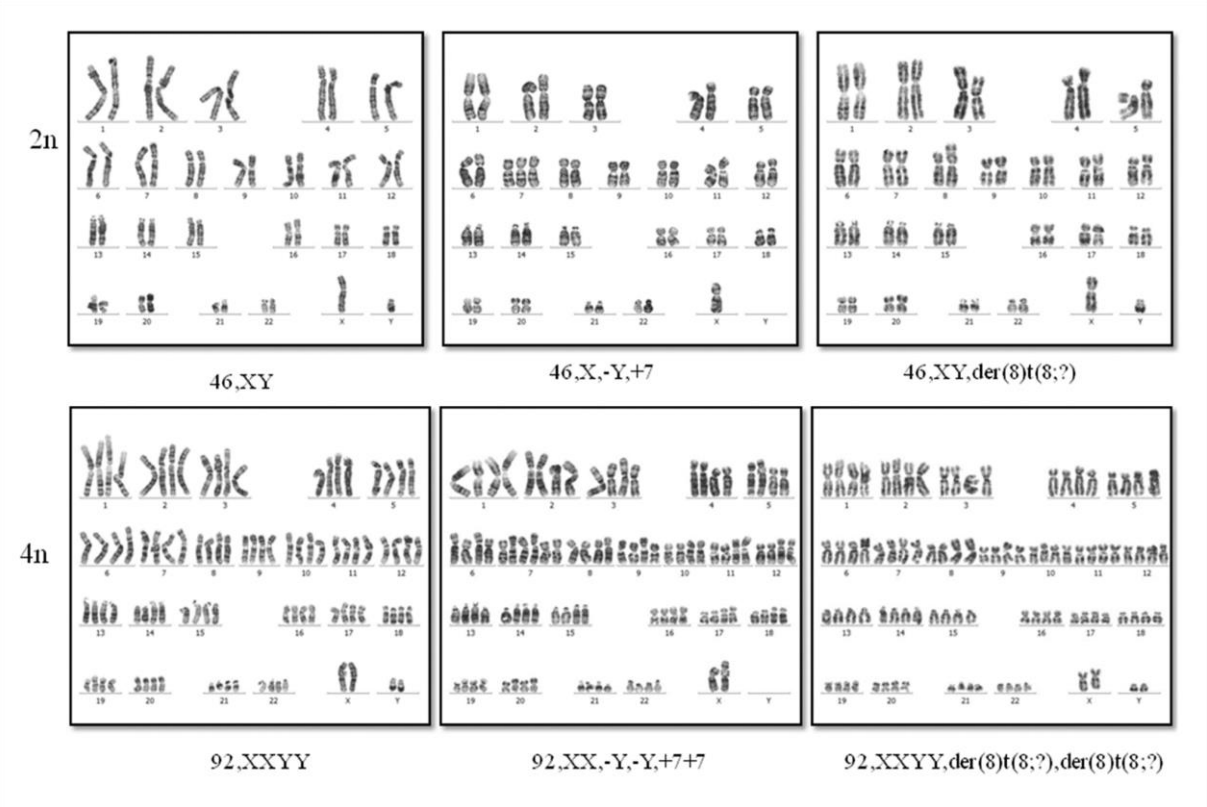

Figure 2 Karyotypic analysis of CCFs. The aberrant karyotypic patterns of CCFs are shown including those with diploid and tetraploid chromosomes.

Table 3 Summary of CCF karyotypes.

Cell	Copy no.	% (no./total screening cells)	Karyotypes	
			Pattern	% (no./total metaphase cells)
CCFs	2n	83% (275/331)	46,XY	35.8% (29/81)
			46,X,-Y,+7	24.7% (20/81)
			46,XY,der(8)t(8;?)	8.6% (21/81)
	4n	16.9% (56/331)	92,XXYY	26% (21/81)
			92,XXYY,der(8)t(8;?), der(8)t(8;?)	3.7% (3/81)
			92,XX,-Y,-Y,+7,+7	1.2% (1/81)
NLF	2n	100%	46,XY	56.3% (9/16)
			45,X,-Y	43.7% (7/16)
SF	2n	100%	46,XY	100% (20/20)

Detection of PN in CCFs and fibroblast embedded within B149 CCA tissues

The result revealed that *PN* could be expressed in CCFs since the early passage (passage 6th) until the late passage of the primary culture fibroblast (passage 16th) (Figure 3A and 3B). In contrast, *PN* showed no expression in all CCA cell lines. In correspondent to these findings, the immunohistochemical stating against PN in CCA tissue exhibited the presence of PN only in the fibroblasts within the cancerous area (Figure 3D) while cancer cells and other stromal cells showed no expression of PN. In addition, the hepatocytes and the stromal cells in the non-tumorigenic adjacent area revealed no PN (Figure 3C).

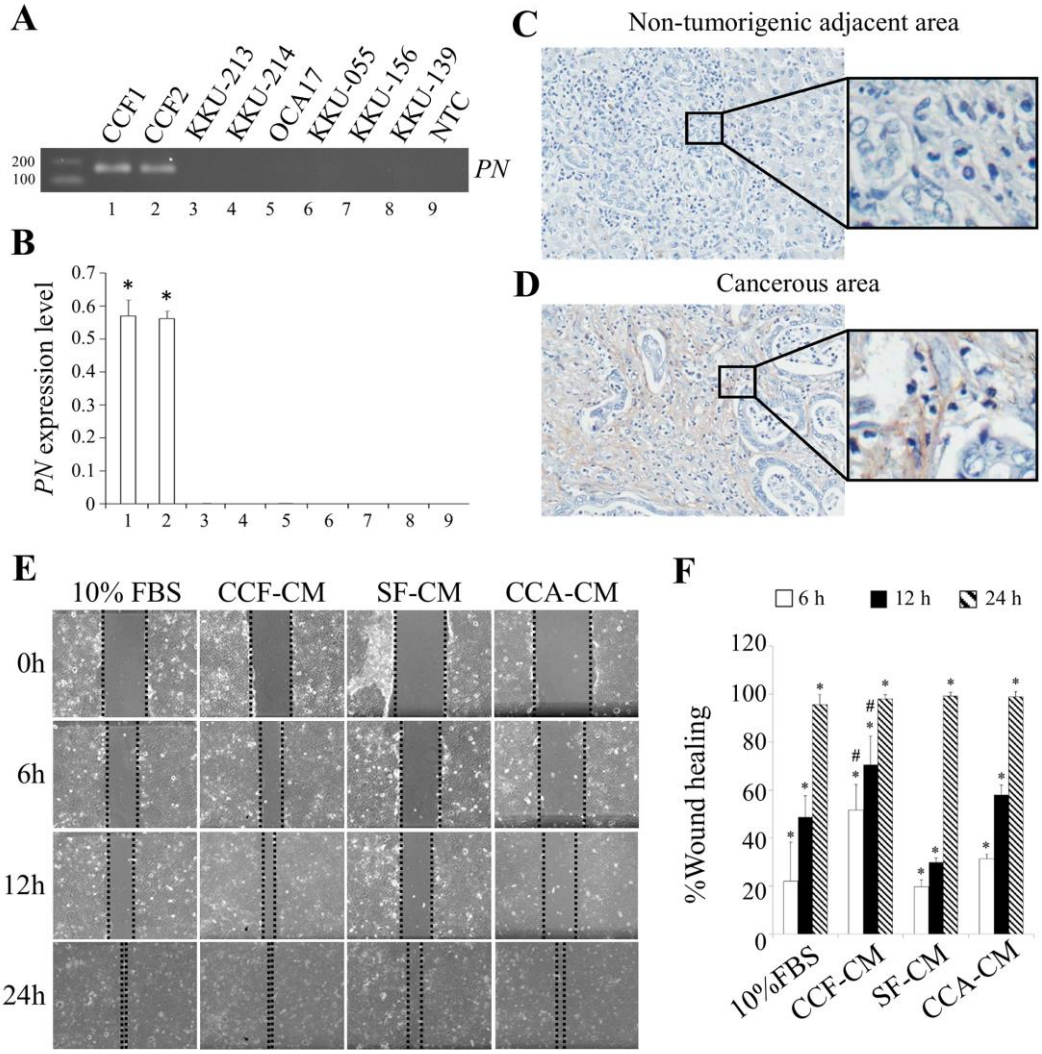

Figure 3 The expression of PN in CCFs and CCFs-CM promotes KKU-213 CCA cell migration. (A) CCFs were expressed *PN* as detected by conventional PCR as compared to no PN in all CCA cell lines. **(B)** The densitometry analysis of PCR product bands. Immunohistochemistry of PN **(C)** the normal adjacent areas and **(D)** cancerous area of CCA tissue. **(E)** Migration assay of CCA cells induced by CCFs-CM. The scratched KKU-213 cells were treated with CCF-CM and the narrowing of the lesion was measured at 0 h, 6 h, 12 h and 24 h compared with those treated with SF-CM. The complete media and KKU-213-CM were used as the negative and positive control, respectively. The microscopic pictures showing the width of the wound at the starting and the ending time point of each treatment condition. **(F)** Percentage of wound healing assay induced by different fibroblast CM. Bar graphs represent the mean ± SD of the % wound healing. *$p<0.05$ compared to that of complete media treatment, # $p<0.05$ compared to that of SF-CM treatment.

Wound healing induction of CCF conditioned-medium

CCFs were maintained up to not more than 20 passages. CCFs-CM induced KKU-213 cancer cells migration ability was checked for the stability of activated phenotypes compared with 10% FBS DMEM medium, SF-CM, and KKU-213-CM treatment (Figure 3E and 3F). The tumorigenic induction potential of CCFs was explored by treating KKU-213 CCA cells with 24-h CM collected from the cultured CCFs. The induced-wound CCA cell layer was stimulated their migration towards each other between the two edges which represent a process of healing by different types of CM. After 6 h of CM treatment, CCF-CM could induce more migration of cancer cells observed by the narrower of the wound than the conditions of treatment with SF-CM. This effect was clearly seen when the cells were induced migration until 12 h of treatment and exhibited the statistically significant difference of cell migration capacity compared to the cells treated with SF-CM and the negative control condition using fresh culture media. These results suggest the migration induction effect of CCF whereas the substances from NFs did not have this function. Even though CM from cancer cells themselves could induce CCA cell migration with statistical significance compared to the control 10% FBS complete medium treatment condition, but not as compared to SF-CM treatment.

IL-6 and HGF expressions in CCFs

Interleukin-6 (*IL-6*) and hepatocyte growth factor (*HGF*) located in the chromosome 7 were detected their higher expression levels in CCFs as compared to those in normal fibroblasts by PCR (Figure 4A and 4B). The expression levels of these 2 genes were not exhibited in CCA cell lines (KKU-213 and KKU-055). IL-6 secreted in CM were further investigated by ELISA. The ELISA results were clearly showed that IL-6 levels were higher in CCFs-CM than pooled SFs-CM (Figure 4C).

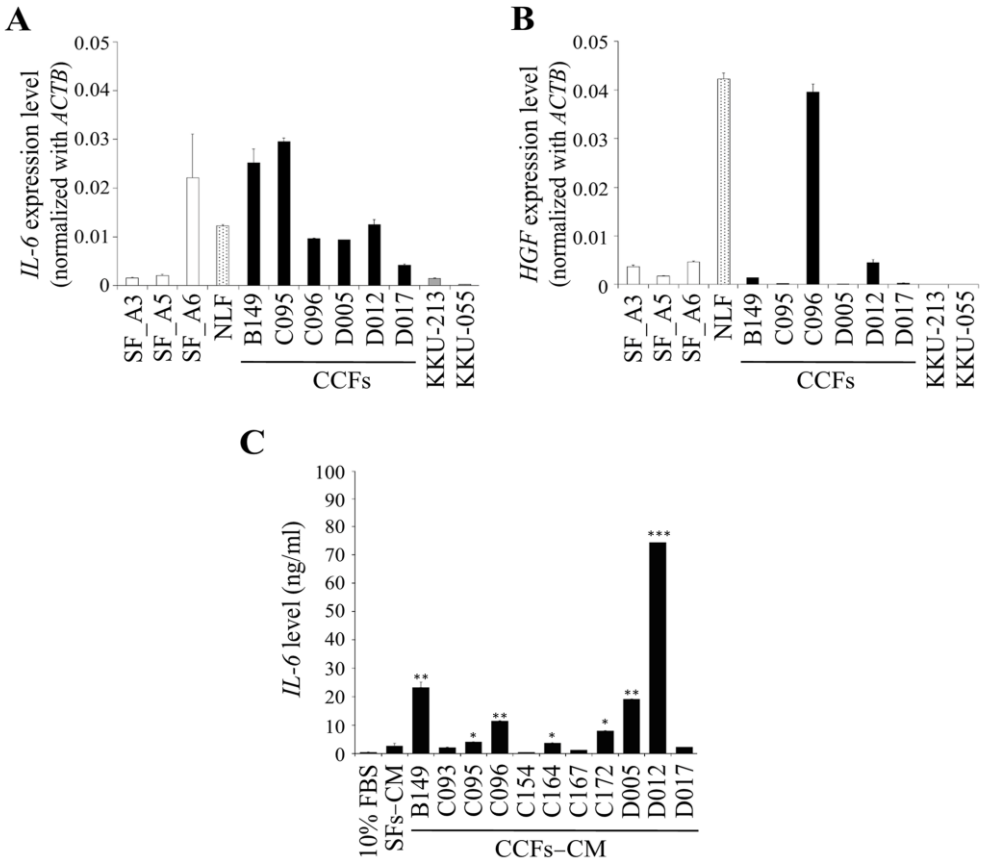

Figure 4 The expression levels of IL-6 and HGF in CCFs. (A) *IL-6* and **(B)** *HGF* in CCFs were detected by real time PCR compared to SFs, NLF and KKU-213 and KKU-055 CCA cell lines. Bars represent mean ± SD of gene expression level in term of $2^{-\Delta Cp}$ using the level of β-actin (*ACTB)* as the internal control. **(C)** ELISA showed expression levels of IL-6 in CCF-CM, pooled SFs-CM and NLF-CM. Bars represent mean ± SD. *p<0.05, **p<0.01, ***p<0.001 compared to that of SFs-CM.

DISCUSSION

There are strong evidences indicated that cancer-associated fibroblasts in CCA have different phenotypes from fibroblasts associated with normal epithelium (Sha *et al.*, 2018; Utispan *et al.*, 2010). Gene expression patterns in cancer-associated fibroblasts have recently been investigated to have abnormalities leading to the increased production of secreted tumorigenic proteins which can promote the aggressiveness of bile duct cancer or CCA (Utispan *et al.*, 2010). CCA fibroblasts have recently been checked for the aberrant microRNA to control the expression of tumor-promoting proteins (Utaijaratrasmi *et al.*, 2018). In this present study, primary culture fibroblasts isolated from CCA tissues, or CCFs, were characterized by the chromosomal aberrations, specific protein productions, and biological functions that induce cancer cell migration.

The characterization of CCFs was confirmed with findings from previous publications to have the fibroblast-liked morphology, absence of CK7, CK19, and the presence of VIM and ASMA (Utaijaratrasmi *et al.*, 2018; Utispan *et al.*, 2010). The absence of epithelial protein CK19 ensured the purity of the isolated primary culture CCFs without epithelial cancer cell contamination. The positive staining of VIM and ASMA indicated the mesenchymal origin and activated phenotype of primary culture CCFs. Though CK7 and CK19 were reported to detect in biliary epithelial cancer cells (Massani *et al.*, 2013), our results exhibited higher level of CK19 than CK7 in KKU-213, OCA17, and KKU-156 CCA cell lines. In the opposite way, KKU-214, KKU-156 and KKU-139 CCA cell lines showed higher level of CK7 than CK19. CCFs had very low expression of *CK* and confirmed to have no protein level detected by immunocytochemistry which supported by the similar pattern in primary culture fibroblasts from CCA tissues (Utaijaratrasmi *et al.*, 2018). PN expression was observed solely in stromal fibroblasts of CCA, but not in any cancer cells or immune cells (Utispan *et al.*, 2010). In addition, the isolated primary culture CCFs obtained herein have been shown to have PN expression. The absence of PN in all CCA cell lines confirmed the finding by immunohistochemical staining of CCA tissues which was the origin of the primary culture CCFs. PN activates CCA cell migration through integrin receptor and mediates epithelial to mesenchymal transition leading to cancer progression (Sonongbua *et al.*, 2020; Utispan *et al.*, 2012).

The genetic alterations in the stromal CAFs has been exhibited to occur in concurrent but independent to the genetic alterations in cancer cells (Moinfar *et al.*, 2000). The evidence suggests that the genetic alterations in the stromal cells may precede genotypic changes in the epithelial cells. Breast cancer-associated fibroblasts derived from BRCA1/2-related and sporadic breast carcinomas have also been reported to carry a certain set of chromosomal aberration with LOH at a frequency similar to that observed in the epithelial components (Weber *et al.*, 2006). The frequent somatic mutations in *TP53* and *PTEN* have been reported in fibroblasts associated with breast cancer (Kurose *et al.*, 2002; Patocs *et al.*, 2007). The results of high-resolution DNA copy number analysis to murine stromal DNA isolated from human xenograft tumors including breast cancer and colon cancer samples showed that numerous amplifications and deletions were found within the host stromal microenvironment suggestion that alterations in host DNA copy number can occur and may play a significant role in modifying tumor-stromal interactions (Pelham *et al.*, 2006). These are in concert with our findings which is the first report in CCA that the fibroblasts in this cancer had chromosomal aberration.

The data presented herein exhibited for the first time the chromosomal alterations in CCFs rather than the aberration of chromosome 17 as previously reported (Matsumoto *et al.*, 2003). The abnormalities of chromosome copy numbers, chromosomal translocations and increasing and the absence of one chromosome number were demonstrated in this present study. Since the presence of several cancer-related genes on chromosome 7 encoded tumor promoting proteins including interleukin-6 (IL-6) and hepatocyte growth factor (HGF), the findings that chromosome 7 was presented as the trisomy in the diploid chromosome and as well as in the tetraploid chromosome of CCFs are of great interest. These abnormalities may lead to the increased production of IL-6 and HGF. IL-6 has been reviewed as the important inflammatory cytokines involving in the carcinogenesis of CCA (Al-Bahrani *et al.*, 2013). IL-6 engages its receptor and consequently activates several signaling pathways in particular PI3 kinase, JAK/STAT, p38 MAP kinase and others that ultimately lead to cell proliferation, protection from apoptosis and increased metastatic potential which can ultimately help cancer cell to proliferate, migration, and invasion (Johnson *et al.*, 2012). For

HGF, the in vitro study showed that HGF promotes CCA cell invasiveness through dyslocalization of E-cadherin and induction of cell motility (Menakongka and Suthiphongchai, 2010). The importance of HGF in CCA has been well reviewed that c-MET, the receptor of HGF, is proposed to be the target for CCA treatment (Labib *et al.*, 2019). In addition, the elevated plasma IL-6 was reported with the increased risk of advanced fibrosis in liver fluke *Opisthorchis viverrini-related CCA* (Sripa *et al.*, 2012). As the study in our lab supported the findings of increasing of secreted IL-6 from CCA-derived fibroblasts.

In conclusion, the present study exhibits the chromosomal abnormalities of fibroblasts associated in CCA tissues. The potential of these abnormalities to be one of the underlying mechanisms to explain the tumorigenic phenotype of cancer-associated fibroblasts is proposed. However, the epigenetic changes and/or microRNA alterations in the stromal cells of CCA are recently proposed (Utaijaratrasmi *et al.*, 2018). The more understanding towards CCA-derived fibroblasts will help design the technique to inhibit them efficiently. As previous report, regarding using navitoclax induced apoptosis of only fibroblasts in CCA in mouse and rat models which is due to the absence of Mcl-1 gene expression in only fibroblasts within CCA tissues (Mertens *et al.*, 2013). The obtained results showed the promising benefit of destroying fibroblasts in the tumor microenvironment leading to the unsuitable extracellular matrix favoring tumor growth, survival, migration and invasion as a general strategy to attack solid tumors.

ACKNOWLEDGEMENTS AND FUNDING

This work has been supported by Thailand Research Fund, grant number RSA5480003 and Research Grant, Faculty of Medicine Siriraj Hospital, Mahidol University (R015633013).

AUTHORS' CONTRIBUTIONS

ST and PU carried out the whole cellular and molecular studies and ST draft the manuscript. WH and PJ participated in karyotype analysis. KV and SW participated in primary fibroblast cell culture. NK and SC performed hepatectomy and surgical manipulation for fresh CCA tissues. PT participated in study design, lab suggestion, and manuscript criticism. CT was responsible for study design, study coordination, interpretation of results, drafted and revised the manuscript. All authors read and approved the final manuscript.

COMPETING INTERESTS

The authors declare that they have no competing interests.

REFERENCES

Al-Bahrani R, Abuetabh Y, Zeitouni N, Sergi C. Cholangiocarcinoma: risk factors, environmental influences and oncogenesis. Ann Clin Lab Sci. 2013;43(2):195-210.

Corver WE, Ter Haar NT, Fleuren GJ, Oosting J. Cervical carcinoma-associated fibroblasts are DNA diploid and do not show evidence for somatic genetic alterations. Cell Oncol (Dordr). 2011;34(6):553-563.

Fukino K, Shen L, Patocs A, Mutter GL, Eng C. Genomic instability within tumor stroma and clinicopathological characteristics of sporadic primary invasive breast carcinoma. JAMA. 2007;297(19):2103-2111.

Hosein AN, Wu M, Arcand SL, Lavallee S, Hebert J, Tonin PN, Basik M. Breast carcinoma-associated fibroblasts rarely contain *p53* mutations or chromosomal aberrations. Cancer Res. 2010;70(14):5770-5777.

Ishiguro K, Yoshida T, Yagishita H, Numata Y, Okayasu T. Epithelial and stromal genetic instability contributes to genesis of colorectal adenomas. Gut. 2006;55(5):695-702.

Jin G, Kim AJ, Jeon H-S, Choi JE, Kim DS, Lee EB, Cha SI, Yoon GS, Kim CH, Jung TH, *et al*. PTEN mutations and relationship to *EGFR*, *EGBB2*, *KRAS*, and *TP53* mutations in non-small cell lung cancers. Lung Cancer. 2010;69(3) 279-283.

Johnson C, Han Y, Hughart N, McCarra J, Alpini G, Meng F. Interleukin-6 and its receptor, key players in hepatobiliary inflammation and cancer. Transl Gastrointest Cancer. 2012;1(1):58-70.

Labib PL, Goodchild G, Pereira SP. Molecular pathogenesis of cholangiocarcinoma. BMC Cancer. 2019;19(1):185.

Massani M, Stecca T, Fabris L, Caratozzolo E, Ruffolo C, Furlanetto A, Morton S, Cadamuro M, Strazzabosco M, Bassi N. Isolation and characterization of biliary epithelial and stromal cells from resected human cholangiocarcinoma: a novel *in vitro* model to study tumor-stroma interactions. Oncol Rep. 2013;30(3):1143-1148

Matsumoto N, Yoshida T, Okayasu I. High epithelial and stromal genetic instability of chromosome 17 in ulcerative colitis-associated carcinogenesis. Cancer Res. 2003;63(19):6158-6161.

Menakongka A, Suthiphongchai T. Involvement of PI3K and ERK1/2 pathways in hepatocyte growth factor-induced cholangiocarcinoma cell invasion. World J Gastroenterol. 2010;16(6):713-722.

Mertens JC, Fingas CD, Christensen JD, Smoot RL, Bronk SF, Werneburg NW, Gustafson MP, Dietz AB, Roberts LR, Sirica AE, *et al.* Therapeutic effects of deleting cancer-associated fibroblasts in cholangiocarcinoma. Cancer Res. 2013;73(2):897-907.

Moinfar F, Man YG, Arnould L, Bratthauer GL, Ratschek,M, Tavassoli FA. Concurrent and independent genetic alterations in the stromal and epithelial cells of mammary carcinoma: implications for tumorigenesis. Cancer Res. 2000;60(9):2562-2566.

Patocs A, Zhang L, Xu Y, Weber F, Caldes T, Mutter GL, Platzer P, Eng C. Breast-cancer stromal cells with TP53 mutations and nodal metastases. N Engl J Med. 2007;357(25):2543-2551.

Pelham RJ, Rodger L, Hall I, Lucito R, Nguyen KC, Navin N, Hicks J, Mu D, Powers S, Wigler M, *et al.* Identification of alterations in DNA copy number in host stromal cells during tumor progression. Proc Natl Acad Sci U S A. 2006;103(52):19848-19853.

Polyak K, Haviv I, Campbell IG. Co-evolution of tumor cells and their microenvironment. Trends Genet. 2009;25(1):30-38.

Qiu W, Hu M, Sridhar A, Opeskin K, Fox S, Shipitsin M, Trivett M, Thompson ER, Ramakrishna M, Gorringe KL, *et al.* No evidence of clonal somatic genetic alterations in cancer-associated fibroblasts from human breast and ovarian carcinomas. Nat Genet. 2008;40(5):650-655.

Sha M, Jeong S, Qiu BJ, Tong Y, Xia L, Xu N, Zhang JJ, Xia Q. Isolation of cancer-associated fibroblasts and its promotion to the progression of intrahepatic cholangiocarcinoma. Cancer Med. 2018;7(9):4665-4677.

Sonongbua J, Siritungyong S, Thongchot S, Kamolhan T, Utispan K, Thuwajit P, Pongpaibul A, Wongkham S, Thuwajit C. Periostin induces epithelialtomesenchymal transition via the integrin alpha5beta1/TWIST2 axis in cholangiocarcinoma. Oncol Rep. 2020;43(4):1147-1158.

Sripa B, Thinkhamrop B, Mairiang E, Laha T, Kaewkes S, Sithithaworn P, Periago MV, Bhudhisawasdi V, Yonglitthipagon P, Mulvenna J, *et al.* Elevated plasma IL-6 associates with increased risk of advanced fibrosis and cholangiocarcinoma in individuals infected by Opisthorchis viverrini. PLoS Negl Trop Dis. 2012;6(5):e1654.

Thongchot S, Ferraresi A, Vidoni C, Loilome W, Yongvanit P, Namwat N, Isidoro C. Resveratrol interrupts the pro-invasive communication betwwen cancer associated fibroblasts and cholangiocarcinoma cells. Cancer Lett. 2018;430:160-171.

Utaijaratrasmi P, Vaeteewoottacharn K, Tsunematsu T, Jamjantra P, Wongkham S, Pairojkul C, Khuntikeo N, Ishimaru N, Sirivatanauksorn Y, Pongpaibul A, *et al.* The microRNA-15a-PAI-2 axis in cholangiocarcinoma-associated fibroblasts promotes migration of cancer cells. Mol Cancer. 2018;17(1):10.

Utispan K, Sonongbua J, Thuwajit P, Chau-In S, Pairojkul C, Wongkham S, Thuwajit C. Periostin activates integrin alpha5beta1 through a PI3K/AKTdependent pathway in invasion of cholangiocarcinoma. Int J Oncol. 2012;41(3):1110-1118.

Utispan K, Thuwajit P, Abiko Y, Charngkaew K, Paupairoj A, Chau-in S, Thuwajit C. Gene expression profiling of cholangiocarcinoma-derived fibroblast reveals alterations related to tumor progression and indicates periostin as a poor prognostic marker. Mol Cancer. 2010;9:13.

Valkenburg KC, de Groot AE, Pienta KJ. Targeting the tumour stroma to improve cancer therapy. Nat Rev Clin Oncol. 2018;15(6):366-381.

Weber F, Shen L, Fukino K, Patocs A, Mutter GL, Caldes T, Eng C. Total-genome analysis of BRCA1/2-related invasive carcinomas of the breast identifies tumor stroma as potential landscaper for neoplastic initiation. Am J Hum Genet. 2006;78(6):961-972.